

This is the accepted manuscript made available via CHORUS. The article has been published as:

# Dependence of $T_{\{c\}}$ on the $q$ - $\omega$ structure of the spin-fluctuation spectrum

Thomas Dahm and D. J. Scalapino

Phys. Rev. B **97**, 184504 — Published 14 May 2018

DOI: [10.1103/PhysRevB.97.184504](https://doi.org/10.1103/PhysRevB.97.184504)

# Dependence of $T_c$ on the $q - \omega$ structure of the spin-fluctuation spectrum

Thomas Dahm

*Universität Bielefeld, Fakultät für Physik,  
Postfach 100131, D-33501 Bielefeld, Germany*

D.J. Scalapino

*Department of Physics, University of California,  
Santa Barbara, CA 93106-9530, USA*

A phenomenological spin-fluctuation analysis<sup>1</sup>, based upon inelastic neutron scattering (INS) and angular resolved photoemission spectroscopy (ARPES) data for YBCO<sub>6.6</sub> ( $T_c = 61K$ ), is used to calculate the functional derivative of the d-wave eigenvalue  $\lambda_d$  of the linearized gap equation with respect to the imaginary part of the spin susceptibility  $\chi''(q, \omega)$  at 70K. For temperatures near  $T_c$ , the variation of  $T_c$  with respect to  $\chi''(q, \omega)$  is proportional to this functional derivative. We find that above an energy  $\sim 4T_c$  the functional derivative becomes positive so that adding spin-fluctuation spectral weight at higher frequencies leads to an increase in  $T_c$ . The strongest pairing occurs for large momentum transfers and small momentum spin-fluctuations suppress the pairing.

For the traditional electron-phonon driven superconductors, the Eliashberg theory for the transition temperature  $T_c$  depends upon the spectral function of the effective interaction  $\alpha^2 F(\omega)$  due to the exchange of phonons and the Coulomb pseudo potential  $\mu^{*2,3}$ . Electron tunneling measurements provided experimental results for these quantities which were used to calculate  $T_c$ <sup>4</sup>. Questions then arose as to how the different frequency regions contributed to  $T_c$ . In order to understand this, Bergmann and Rainer<sup>5</sup> used electron tunneling data and calculated the functional derivative of  $T_c$  with respect to  $\alpha^2 F(\omega)$ . They found that while all parts of the phonon spectrum contributed to  $T_c$ ,  $\delta T_c / \delta \alpha^2 F(\omega)$  peaked for  $\omega \sim 7T_c$ , falling off at higher frequencies. In contrast to the electron-phonon case, the pairing interaction in the cuprates has an important momentum dependence so that one would like to understand how both different  $q$  and  $\omega$  regions contribute to  $T_c$ . While one lacks an equivalent Eliashberg theory, fluctuation exchange (FLEX) calculations of the variation of  $T_c$  with changes in the  $q - \omega$  spin-fluctuation spectral weight for the 2D Hubbard model have been reported<sup>6</sup>. Here we take a more phenomenological approach and explore how inelastic neutron scattering (INS) data<sup>7-10</sup> for the dynamic spin susceptibility  $\chi''(q, \omega)$  along with angular resolved photoemission (ARPES) results<sup>11,12</sup> for YBCO<sub>6.6</sub> can provide insight into how different parts of the  $q$  and  $\omega$  dependent spin-fluctuation spectrum contribute to the pairing. We find for YBCO<sub>6.6</sub> that there is pair breaking for  $\omega \lesssim 25$  meV and that the dominant pairing strength comes from the upper branch of the YBCO<sub>6.6</sub> spin-fluctuation spectrum.

Within the spin-fluctuation framework, the diagrams for the one-electron self-energy and the linearized gap equation are shown in Figure 1. Here the wiggly line represents the effective interaction

$$V_{\text{eff}}(q, \omega) = \frac{3}{2} \bar{U}^2 \chi(q, \omega) \quad (1)$$

with  $\chi(q, \omega)$  the  $q$  and  $\omega$  dependent spin susceptibility measured by inelastic neutron scattering<sup>7-10</sup>. Here, as in Ref. [1], the parameterized form for  $\chi(q, \omega)$  that we will use describes the odd symmetry channel with respect to the interchange of adjacent  $\text{CuO}_2$  bilayers. This is the channel that contains the spin resonance and the one whose  $q$  and  $\omega$  contributions to the pairing we will examine. The solid lines represent the one-electron Green's function  $G(k, \omega)$  with the one-loop self-consistent self-energy illustrated in Fig. 1a. In our calculations, the imaginary parts of the one-loop self-energies for the antibonding

(A) and bonding (B) two-layer bands are given by

$$\text{Im}\Sigma_{A,B}(k, \omega) = \frac{1}{N} \sum_Q \int_{-\infty}^{\infty} \frac{d\Omega}{\pi} [n(\Omega) + f(\Omega - \omega)] \text{Im}V_{\text{eff}}(Q, \Omega) \text{Im}G_{B,A}(k - Q, \omega - \Omega) \quad (2)$$

Here  $n$  and  $f$  are the Bose and Fermi functions, respectively, and  $Q$  is summed over the 2D Brillouin zone. The odd symmetry of  $\chi(q, \omega)$  channel couples  $\Sigma_A$  to  $G_B$  and  $\Sigma_B$  to  $G_A$ . The real parts of  $\Sigma_{A,B}$  are evaluated by a Kramers-Kronig transformation.

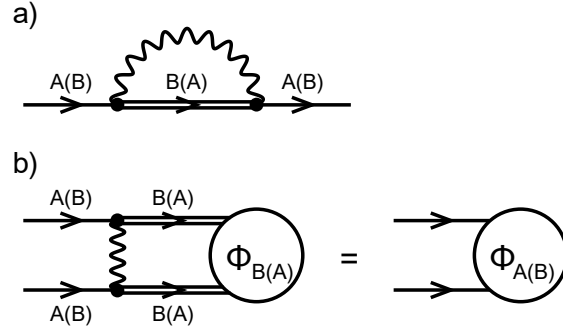


FIG. 1. a) One loop self-energy diagram. Here the wiggly line represents the interaction, Eq. (1), and the solid line represents the dressed single particle Green's function.; b) The Bethe-Salpeter linearized gap diagram.

The dispersion relations of the unrenormalized electron bands  $\varepsilon^{A,B}(k)$  of the two-layer  $\text{YBa}_2\text{Cu}_3\text{O}_{6.6}$  system are modeled by tight binding parameters and a chemical potential. In the iterative calculation of the self-energy, these parameters are adjusted to preserve the observed ARPES bonding and antibonding Fermi surfaces of the dressed electrons. The coupling  $\bar{U}$  was chosen to fit the observed nodal Fermi velocity<sup>1</sup>, but its precise magnitude plays a negligible role in the  $q$  and  $\omega$  dependence of the functional derivative.

The imaginary part of the linearized gap equation, Fig. 1b, is given by

$$\frac{1}{\pi N} \sum_{k'} \int_{-\infty}^{\infty} d\omega' [n(\omega - \omega') + f(-\omega')] \text{Im}V_{\text{eff}}(k - k', \omega - \omega') \text{Im} \left( \frac{\phi_{B,A}(k', \omega')}{(\omega' Z_{BA})^2 - (\tilde{\varepsilon}^{B,A}(k))^2} \right) = \lambda_d(T) \text{Im}\phi_{A,B}(k, \omega) \quad (3)$$

with

$$\omega Z_{B,A}(k, \omega) = \omega - \frac{1}{2} (\Sigma_{B,A}(k, \omega) - \Sigma_{B,A}^*(k, -\omega)) \quad (4)$$

and

$$\tilde{\varepsilon}^{\text{B,A}}(k) = \varepsilon^{\text{B,A}}(k) + \frac{1}{2} (\Sigma_{\text{B,A}}(k, \omega) + \Sigma_{\text{B,A}}^*(k, -\omega)) \quad (5)$$

The eigenfunction of Eq. (3) with the largest low temperature eigenvalue has  $d$ -wave symmetry and its eigenvalue  $\lambda_d(T)$  approaches 1 as  $T$  goes to  $T_c$ . In the following we will calculate the functional derivative of  $\lambda_d(T)$  with respect to  $\text{Im}\chi(q, \omega)$  for momentum  $q$  along the diagonal of the Brillouin zone, using INS results for YBCO<sub>6.6</sub> measured at  $T = 70\text{K}$ . The  $T_c$  of YBa<sub>2</sub>Cu<sub>3</sub>O<sub>6.6</sub> is 61K and for  $T$  near  $T_c$ , the variation of  $T_c$  with respect to  $\text{Im}\chi(q, \omega)$  is proportional to  $\delta\lambda_d/\delta\text{Im}\chi(q, \omega)$ . To calculate  $\delta\lambda_d/\delta\text{Im}\chi(q, \omega)$  at  $\omega_0$  and  $q_0$ , we set  $\text{Im}\tilde{\chi}(q, \omega) = \text{Im}\chi(q, \omega) + a\delta(\omega - \omega_0)\delta(q - q_0)$  and numerically evaluated  $(\tilde{\lambda}_d - \lambda_d)/a$ . Here  $a = 0.1$  is small compared to the integrated spectral weight over a phase space region  $\Delta q \Delta \omega$  with  $\frac{\Delta q}{q} = \frac{\Delta \omega}{\omega} = 0.01$ .

A plot of a parameterized fit<sup>1</sup> of the INS data showing  $\chi''(q, \omega, 70\text{K})$  for YBCO<sub>6.6</sub> at  $T = 70\text{K}$  is shown in Fig. 2a. For this underdoped cuprate there is a clear pseudogap and the spin-fluctuation spectrum can be considered as having upper and lower branches. In Fig. 2b a similar plot of  $\chi''(q, \omega, 5\text{K})$  for  $T = 5\text{K}$  shows the development of the hour-glass dispersion and spin resonances in the superconducting state. The functional derivative  $\delta\lambda_d/\delta(\text{Im}\chi(q, \omega, 70\text{K}))$  plotted in Fig. 3 provides a map showing how different regions of the  $q - \omega$  phase space contribute to the pairing. The strongest pairing occurs for large momentum transfers with frequencies extending from  $\sim 40\text{meV}$  to several hundred meV. At high frequencies for  $q$  along the diagonal, the functional derivative varies as  $-\cos(q)/\omega$ . At frequencies lower than  $\sim 25\text{meV}$ , adding additional spin-fluctuation spectral weight reduces  $\lambda_d$  corresponding to a suppression of  $T_c$ . This reflects the well known pair breaking effects of low frequency spin fluctuations<sup>13</sup>. As opposed to the phonon case where fluctuations at all frequencies contribute to  $T_c$ , the low frequency spin fluctuations act as static magnetic impurities and suppress  $T_c$ . At small momentum transfers, the spin-fluctuations predominantly scatter pairs between regions of the Fermi surface where the  $d$ -wave gap has the same sign and the functional derivative becomes negative. As seen from the dashed curve of Fig3b for  $q = (0.6\pi, 0.6\pi)$ , even at large frequencies this effect of the  $d$ -wave form factor leads to negligible pairing. Overall it is clear that the dominant contribution to the pairing is coming from the upper branch of the spin fluctuations.

The product of  $\chi''(q, \omega, 70\text{K})$  times the functional derivative  $\delta\lambda_d/\delta\chi''(q, \omega)$  is shown in

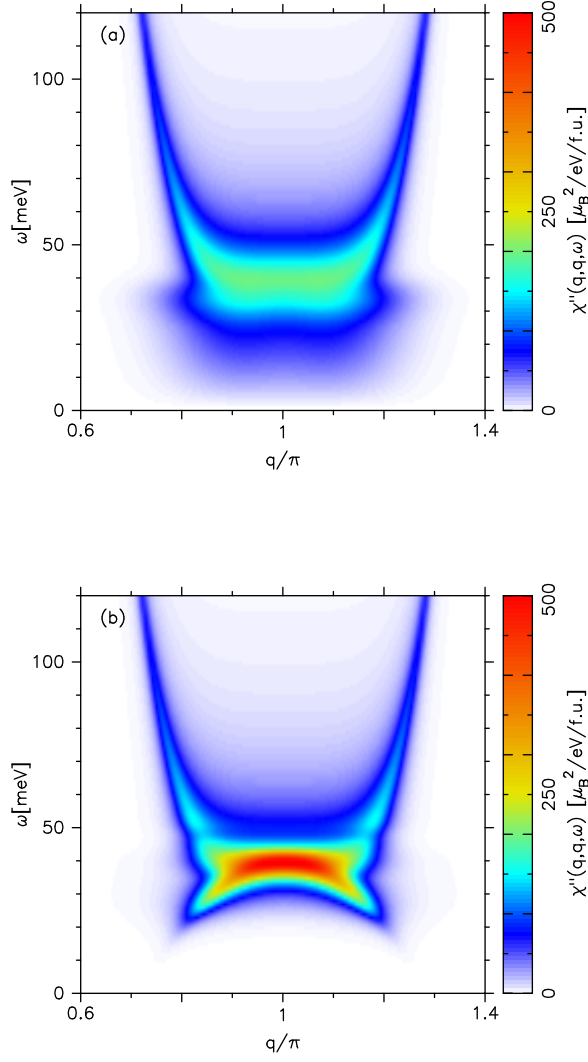


FIG. 2. (a) Parameterization of  $\chi''(q, \omega, 70\text{K})$  obtained from inelastic neutron scattering on YBCO<sub>6.6</sub> at  $T = 70\text{K}$  (see supplementary material of Ref.<sup>1</sup>). Here  $q$  runs along the diagonal direction of the Brillouin zone, i.e.  $q_x = q_y = q$ . (b) A similar plot of  $\chi''(q, \omega, 5\text{K})$  for  $T = 5\text{K}$ .

Fig. 4a. This quantity illustrates how different parts of the spectrum contribute to the pairing. The red pairbreaking region below  $\sim 25$  meV in the functional derivative shown in Fig. 3 is not so destructive for superconductivity in YBCO<sub>6.6</sub> because there is not so much weight in  $\chi''(q, \omega, 70\text{K})$  in this frequency region. In this sense the opening of the pseudogap in  $\chi''(q, \omega)$  enhances the pairing. The green region of the functional derivative in Fig. 3 is emphasized by the “upper branch” of the spin-fluctuation spectrum. It is interesting

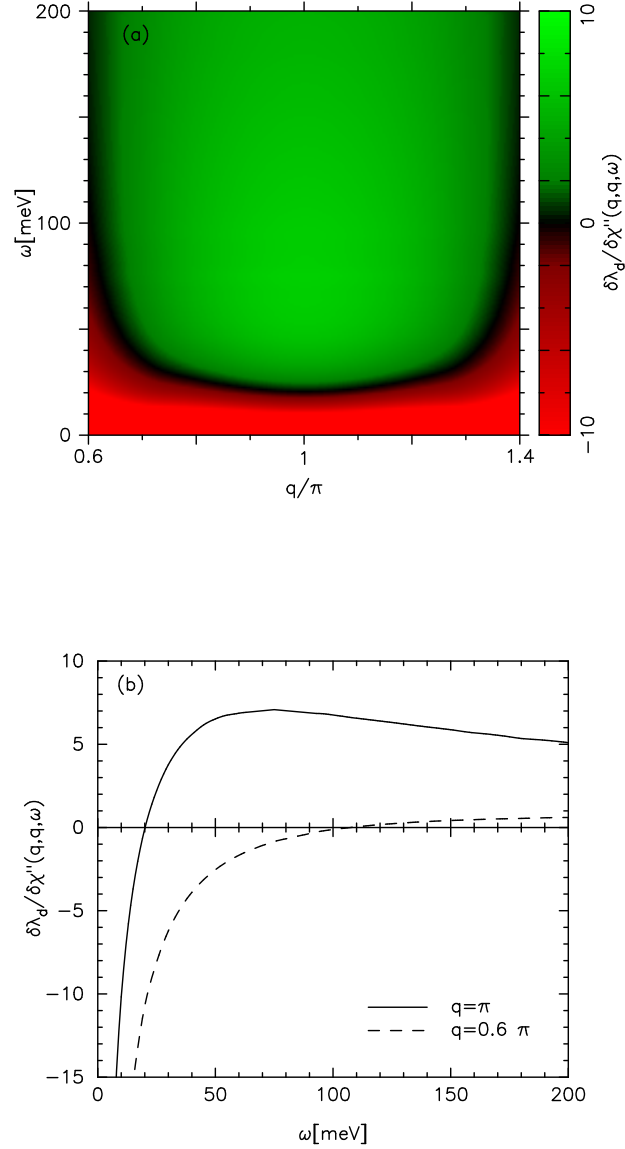


FIG. 3. (a) The functional derivative of the d-wave eigenvalue  $\lambda_d$  with respect to  $\chi''(q, \omega, 70\text{K})$  versus  $\omega$  and  $(q_x = q, q_y = q)$ . The normalization is such that  $\chi''(q, \omega, 70\text{K}) \frac{\delta\lambda_d}{\delta\chi''(q, \omega, 70\text{K})}$  averaged over the  $q - \omega$  phase space shown in the figure is 1. (b) The  $\omega$  dependence of  $\frac{\delta\lambda_d}{\delta\chi''(q, \omega, 70\text{K})}$  for  $q = \pi$  (solid) and  $q = 0.6\pi$  (dashed).

to examine a similar plot in which the functional derivative of Fig. 3 is multiplied by the  $\chi''(q, \omega, T = 5\text{K})$ . As seen in Fig. 2b, when  $T$  decreases from 70K to 5K, the low frequency part of the spin-fluctuation spectral weight decreases and the intensity increases in regions that contribute to the pairing. This behavior is clearly reflected in Fig. 4b. As noted in

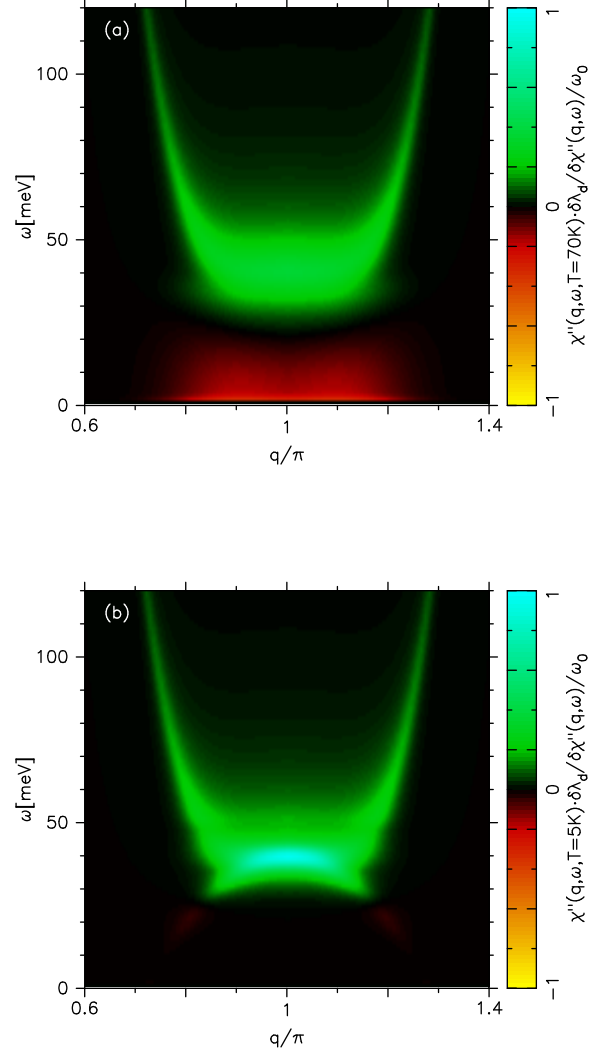


FIG. 4. (a) Plot of  $\chi''(q, \omega, 70\text{K})$  times the functional derivative shown in Fig. 3 divided by  $0.8\pi\omega_0$ . This quantity gives the contribution to the d-wave eigenvalue  $\lambda_d$  from a  $\Delta q \times \Delta\omega$  region of  $(q, \omega)$  phase space for  $T = 70\text{K}$ . (b) A similar plot using the functional derivative computed at  $T = 70\text{K}$  and  $\chi''(q, \omega, T = 5\text{K})$ . These plots illustrate how different parts of the spin-fluctuation spectrum of YBCO<sub>6.6</sub> contribute to  $\lambda_d$ . There is an increase of the pairing strength that occurs as  $T$  drops below  $T_c$  and weight in the spin-fluctuation spectrum shifts to higher frequencies.



Ref.<sup>1</sup>, if  $\text{Im}\chi(q, \omega, 70K)$  is replaced by the 5K INS data  $\text{Im}\chi(q, \omega, 5K)$  in the Bethe-Salpeter equation, one finds an approximate 50% increase in  $\lambda_d$ .

Central to the proposal that antiferromagnetic spin-fluctuations provide the pairing interaction responsible for superconductivity in the cuprate superconductors is the idea that there is a significant coupling between the spins and the doped holes. A consequence of this is that when the system becomes superconducting and a d-wave gap opens in the quasi-particle spectrum, the anti-ferromagnetic spin-fluctuation spectrum will be altered. In the superconducting state, spin-fluctuation spectral weight is shifted up in frequency along with the formation of a spin resonance changing the strength of the pairing interaction. The results shown in Fig. 4 provide evidence that the pairing strength increases below  $T_c$  as spin-fluctuation spectral weight is removed from low frequencies and shifted to frequencies of order  $2\Delta_{\text{max}}$ . One consequence of this is that the magnitude of the d-wave gap will increase more rapidly as  $T$  drops below  $T_c$  and  $2\Delta_{\text{max}}/kT_c$  will be larger than found from predictions based upon a pairing interaction which remains the same below  $T_c$ .

In summary, the  $q$  and  $\omega$  dependence of the functional derivative  $\delta\lambda_d/\delta(\text{Im}\chi(q, \omega))$  of the  $d$ -wave pairing eigenvalue has been calculated for YBCO<sub>6.6</sub>. At small values of  $\omega \lesssim 20$ -25 meV  $\delta\lambda_d/\delta(\text{Im}\chi(q, \omega))$  is negative, reflecting the pair-breaking associated with low energy spin fluctuations. The functional derivative is also negative for smaller values of momentum transfer  $q$  which dominantly connects regions in which the  $d$ -wave gap has the same sign. The functional derivative is positive at large momentum transfer and over a wide range of frequencies above the pair breaking region.

## ACKNOWLEDGMENTS

The authors would like to thank Steve Kivelson and John Tranquada for helpful discussions. DJS was supported by the SciDAC program of the U.S. Department of Energy Division of Materials Sciences and Engineering.

---

<sup>1</sup> T. Dahm, V. Hinkov, S. V. Borisenko, A. A. Kordyuk, V. B. Zabolotnyy, J. Fink, B. Büchner, D. J. Scalapino, W. Hanke, B. Keimer, *Nature Physics* **5**, 217 (2009)

<sup>2</sup> G. M. Eliashberg, *Sov. Phys. JETP* **11**, 696 (1960)

- <sup>3</sup> W. L. McMillan and J. M. Rowell, in *Superconductivity*, edited by R. D. Parks (Dekker, New York, 1969), Vol. I, Chap. 11
- <sup>4</sup> P. B. Allen and R. C. Dynes, *Phys. Rev. B*, 905 (1975)
- <sup>5</sup> G. Bergmann and D. Rainer, *Zeitschrift für Physik*, **263**, 445 (1974)
- <sup>6</sup> P. Monthoux and D.J. Scalapino, *Phys. Rev. B* **50**, 10339 (1994)
- <sup>7</sup> S. M. Hayden, H. A. Mook, P. Dai, T. G. Perring, and F. Dogan, The structure of the high-energy spin excitations in a high-transition-temperature superconductor. *Nature* **429**, 531-534 (2004).
- <sup>8</sup> V. Hinkov, P. Bourges, S. Pailh  s, Y. Sidis, A. Ivanov, C. D. Frost, T. G. Perring, C. T. Lin, D. P. Chen and B. Keimer, Spin dynamics in the pseudogap state of a high-temperature superconductor *Nat. Phys.* **3**, 780-785 (2007).
- <sup>9</sup> H. F. Fong, P. Bourges, Y. Sidis, L. P. Regnault, J. Bossy, A. Ivanov, D. L. Milius, I. A. Aksay, and B. Keimer, Spin susceptibility in underdoped  $\text{YBa}_2\text{Cu}_3\text{O}_{6+x}$ . *Phys. Rev. B* **61**, 14773 (2000).
- <sup>10</sup> P. Bourges, H. F. Fong, L. P. Regnault, J. Bossy, C. Vettier, D. L. Milius, I. A. Aksay, and B. Keimer, High-energy spin excitations in  $\text{YBa}_2\text{Cu}_3\text{O}_{6.5}$ . *Phys. Rev. B* **56**, R11439 (1997).
- <sup>11</sup> S. V. Borisenko, A. A. Kordyuk, V. Zabolotnyy, J. Geck, D. Inosov, A. Koitzsch, J. Fink, M. Knupfer, B. B  chner, V. Hinkov, C. T. Lin, B. Keimer, T. Wolf, S. G. Chiuzb  ian, L. Patthey, and R. Follath, Kinks, nodal bilayer splitting and interband scattering in  $\text{YBa}_2\text{Cu}_3\text{O}_{6+x}$ . *Phys. Rev. Lett.* **96**, 117004 (2006).
- <sup>12</sup> V. B. Zabolotnyy, S. V. Borisenko, A. A. Kordyuk, J. Geck, D. S. Inosov, A. Koitzsch, J. Fink, M. Knupfer, B. B  chner, S.-L. Drechsler, H. Berger, A. Erb, M. Lambacher, L. Patthey, V. Hinkov, and B. Keimer, Momentum and temperature dependence of renormalization effects in the high-temperature superconductor  $\text{YBa}_2\text{Cu}_3\text{O}_{7-\delta}$ . *Phys. Rev. B* **76**, 064519 (2007).
- <sup>13</sup> A. J. Millis, S. Sachdev, and C. M. Varma, *Phys. Rev. B* **37**, 4975 (1988)